SCHD
Structural & Congenital Heart Disease

Tech Science Press

http://doi.org/10.32604/schd.2026.077380

ARTICLE

Integrated Proteomic and Metabolomic Profiling Reveals Impaired Mitochondrial Oxidative Phosphorylation in Hypertrophic Cardiomyopathy

Meng-Zhen Zhang[1,#], Ming Li[2,#], Peng-Ju Wen[1], Yue-Heng Wu[1,*] and Ling Sun[3,*]

[1]Institute of Medical Research, Guangdong Provincial People's Hospital (Guangdong Academy of Medical Sciences), Southern Medical University, Guangzhou, China
[2]Department of Echo Room, Guangdong Provincial People's Hospital (Guangdong Academy of Medical Sciences), Southern Medical University, Guangzhou, China
[3]Department of Pediatric Cardiology, Guangdong Cardiovascular Institute, Guangdong Provincial People's Hospital (Guangdong Academy of Medical Sciences), Southern Medical University, Guangzhou, China
*Corresponding Authors: Yue-Heng Wu. Email: wuyueheng@gdph.org.cn; Ling Sun. Email: sunling@gdph.org.cn
#These authors contributed equally to this work as the first author

Received: 08 December 2025; Accepted: 05 June 2026; Published: 31 July 2026

ABSTRACT: Background: Hypertrophic cardiomyopathy (HCM) is increasingly recognized as a disease of impaired myocardial energetics, but integrated proteomic–metabolomic data from human myocardium are scarce. This study combined quantitative proteomics and untargeted metabolomics to obtain a systems-level view of myocardial remodeling and to identify pathways jointly dysregulated at the protein and metabolite levels. **Methods:** Myocardial tissue from 7 patients with HCM who underwent surgical myectomy and 5 healthy control donors at Guangdong Provincial People's Hospital was analyzed by data-independent acquisition-based quantitative proteomics and Liquid Chromatography-Tandem Mass Spectrometry–based untargeted metabolomics. Differentially expressed proteins (DEPs) and metabolites were identified using predefined fold change and statistical thresholds. Gene Ontology and pathways enrichment analyses were performed, and significantly enriched pathways from proteomics and metabolomics were intersected. **Results:** Proteomic profiling identified 165 DEPs and showed prominent enrichment of mitochondrial and oxidative phosphorylation–related terms, indicating extensive remodeling of respiratory chain complexes. Metabolomic analysis identified nearly 200 differential metabolites, with enrichment in purine metabolism and energy-sensing pathways, including AMPK and cGMP–PKG signaling. Intersecting 77 proteomic and 38 metabolomic pathways yielded seven shared pathways, among which oxidative phosphorylation emerged as a central node. Within this pathway, 23 of 24 proteins were downregulated, ATP5PO was upregulated, and NAD and ADP were decreased, consistent with impaired mitochondrial ATP production. **Conclusion:** Integrated proteomic and metabolomic profiling of HCM myocardium provides convergent evidence that mitochondrial oxidative phosphorylation is a core site of energetic dysfunction, highlighting mitochondrial and energy related pathways as potential targets for future mechanistic and therapeutic studies.

KEYWORDS: Hypertrophic cardiomyopathy; proteomics; metabolomics; mitochondrial dysfunction; oxidative phosphorylation

1 Introduction

Hypertrophic cardiomyopathy (HCM) is a primary myocardial disease characterized by unexplained left ventricular hypertrophy, myocyte disarray, and interstitial fibros. It is an important cause of heart

failure and sudden cardiac death in younger individuals [1]. Beyond structural remodeling, accumulating evidence indicates that impaired myocardial energetics and mitochondrial dysfunction are central features of HCM [2].

With the development of high-throughput technologies, omics studies have begun to elucidate the molecular basis of these abnormalities. Transcriptomic analyses in HCM have revealed changes in genes related to extracellular matrix, inflammation and metabolism, and proteomic studies have reported alterations in contractile and mitochondrial proteins in hypertrophied myocardium [3]. An integrative transcriptome–proteome work have highlighted discrepancies between mRNA and protein levels, suggesting important post-transcriptional regulation [4]. However, most existing studies remain confined to the gene and protein expression layers and provide only indirect inference about functional metabolic consequences. Systematic integration of proteomic and metabolomic data from human HCM myocardium is still lacking.

Proteomics reflects the abundance of enzymes and structural/signal proteins, whereas metabolomics captures the downstream state of metabolic pathways and energy substrates, which are closer to the functional phenotype [5]. Combining proteomics and metabolomics in the same myocardial samples is therefore well suited to bridge altered protein networks with their metabolic output, and to identify pathways that are consistently perturbed at both enzyme and metabolite levels. In a condition such as HCM, where mitochondrial energetics and substrate handling are thought to be profoundly disturbed, a joint proteomic–metabolomic approach may be particularly informative.

In this context, we applied integrated quantitative proteomic and untargeted metabolomic profiling to human HCM and control myocardium to obtain a systems-level view of myocardial remodeling and to identify key metabolic and mitochondrial pathways jointly dysregulated at the protein and metabolite levels.

2 Materials and Methods

2.1 Clinical Sample Collection and Preparation

Human myocardial tissue samples were obtained from seven patients with HCM who underwent surgical myectomy at Guangdong Provincial People's Hospital. The diagnosis of HCM was established according to contemporary guideline criteria based on comprehensive clinical evaluation, including echocardiography and/or cardiac magnetic resonance imaging. Control myocardial samples were obtained from five healthy organ donors with no history of cardiovascular disease, confirmed through standard donor screening. Samples were collected between 2018 and 2020. This retrospective study analyzed frozen myocardial tissue specimens. This is a cross-sectional study, as all samples were collected at a single time point without longitudinal follow-up. Among the seven HCM patients, five were male and two were female, with an age range of 9–52 years. Due to the anonymous nature of organ donor protocols and confidentiality agreements, detailed demographic information (including age and sex) for the five healthy control donors was not available for disclosure. All samples were collected with written informed consent from participants or their legal guardians. The study protocol was approved by the Ethics Committee of Guangdong Provincial People's Hospital (approval No. GDREC2016255H) and conducted in accordance with the Declaration of Helsinki. Immediately after excision, myocardial specimens were rinsed in cold saline, snap frozen in liquid nitrogen, and stored at -80°C until proteomic and metabolomic analysis. For each case, adjacent tissue fragments from the same sample block were used in parallel for protein and metabolite extraction to ensure matched multi-omics profiling.

2.2 Proteomic and Metabolomic Sample Preparation

For proteomic and metabolomic analyses, adjacent pieces of frozen myocardial tissue (~50 mg each) from the same HCM and control samples were processed in parallel to enable matched multi-omics profiling. Samples were kept on dry ice throughout preparation.

For proteomics, myocardial tissue was lysed in urea buffer with protease inhibitors, and protein concentrations were determined by bicinchoninic acid assay. Equal amounts of protein from each sample were reduced, alkylated, and trypsin-digested, and the resulting peptides were desalted and quantified prior to Liquid Chromatography-Tandem Mass Spectrometry (LC–MS/MS) analysis.

For metabolomics, aliquots of the same tissue samples were extracted with cold methanol/water containing 0.02 mg/mL of internal standard (L-2-chlorophenylalanine, CAS: 10389-97-6, exact molecular weight: 199.04 Da), and the supernatants were used for LC–MS/MS profiling. A pooled quality control (QC) sample, prepared by mixing equal volumes of all extracts, was analyzed at regular intervals to monitor analytical stability.

2.3 Proteomic LC–MS/MS Acquisition and Data Processing

Tryptic peptides were reconstituted in 0.1% formic acid in 2% acetonitrile containing indexed retention time (iRT) standards and analyzed by an EASY nLC system (Thermo, USA) coupled to a Trapped Ion Mobility Spectrometry Time-Of-Flight (timsTOF) Pro2 mass spectrometer (Bruker, Germany) in data independent acquisition (DIA PASEF) mode at Majorbio Bio Pharm Technology Co. Ltd. (Shanghai, China). Briefly, a C18 reversed-phase column (75 μm × 25 cm, IonOpticks, USA) was equilibrated with solvent A (2% acetonitrile with 0.1% formic acid) and solvent B (80% acetonitrile with 0.1% formic acid). The peptides were eluted using the following gradient at a flow rate of 250 nL/min: 0–45 min, 3%–28% B; 45–50 min, 28%–44% B; 50–55 min, 44%–90% B; followed by a washing and re-equilibration step. DIA data were acquired over an m/z range of 400–1200 with 64 isolation windows using standard timsTOF Pro2 DIA PASEF settings.

Raw DIA PASEF data were processed with Spectronaut (version 14, Biognosys INC. Switzerland). Retention times were calibrated using iRT peptides. Protein identification and quantification were performed against the human UniProt database with a peptide and protein false discovery rate (FDR) $\leq$ 1%. Only proteins with at least one unique peptide were retained. Label-free quantitative intensities were log2 transformed and normalized. Differentially expressed proteins (DEPs) between HCM and control groups were defined using |fold change (FC)| > 1.0 and $p < 0.05$.

2.4 Metabolomic LC–MS/MS Acquisition and Data Processing

The LC-MS/MS analysis was conducted on a Thermo UHPLC-Q Exactive HF-X system equipped with an ACQUITY HSS T3 column (100 mm × 2.1 mm i.d., 1.8 μm; Waters, USA) at Majorbio Bio-Pharm Technology Co. Ltd. (Shanghai, China). The mobile phases consisted of 0.1% formic acid in water: acetonitrile (95:5, v/v) (solvent A) and 0.1% formic acid in acetonitrile:isopropanol:water (47.5:47.5:5, v/v/v) (solvent B). The flow rate was 0.40 mL/min, and the column temperature was 40°C. Positive ion mode gradient: 0–3 min, B increased from 0% to 20%; 3–4.5 min, B increased from 20% to 35%; 4.5–5 min, B increased from 35% to 100%; 5–6.3 min, B held at 100%; 6.3–6.4 min, B decreased from 100% to 0%; 6.4–8 min, B held at 0%. Negative ion mode gradient: 0–1.5 min, B increased from 0% to 5%; 1.5–2 min, B increased from 5% to 10%; 2–4.5 min, B increased from 10% to 30%; 4.5–5 min, B increased from 30% to 100%; 5–6.3 min, B held at 100%; 6.3–6.4 min, B decreased from 100% to 0%; 6.4–8 min, B held at 0%.

Raw LC–MS data were processed using Progenesis QI (Waters Corporation) for peak detection, alignment, and intensity extraction. Metabolites were annotated by matching accurate mass, retention

time, and MS/MS spectra against the Human Metabolome Database. Data preprocessing on the Majorbio Cloud platform (China, https://www.majorbio.com/tools) included filtering of features detected in <80% of samples, normalization, QC-based filtering, and log10 transformation [6]. Principal Component Analysis (PCA) and Orthogonal Partial Least Squares Discrimination Analysis (OPLS-DA) were performed using the ropls package in R, and differential metabolites between HCM and control groups were defined as those with variable importance in projection (VIP) > 1 and $p < 0.05$ (Student's t-test).

2.5 Functional Enrichment and Integrated Pathway Analysis

Functional enrichment analyses were performed to characterize the biological processes and pathways associated with the observed proteomic and metabolomic changes. For proteomic data, DEPs were subjected to Gene Ontology (GO) enrichment (biological process, cellular component, and molecular function) and Kyoto Encyclopedia of Genes and Genomes (KEGG) pathway analysis using the clusterProfiler package in R [7]. For metabolomic data, differential metabolites were mapped to KEGG pathways and tested for over representation using the KEGG database (http://www.genome.jp/kegg/) [8]. Enriched GO terms and KEGG pathways with $p < 0.05$ were considered significant and were visualized as bar plots or bubble plots. The Pathview package in R was used to project DEPs and metabolites onto the KEGG pathway [9].

2.6 Statistical Analysis

All statistical analyses were performed in R (version 4.3.0). Differential proteins and metabolites were identified using standard univariate tests combined with multiple significance threshold $p < 0.05$. For multivariate analysis, orthogonal partial least squares discriminant analysis (OPLS-DA) and partial least squares discriminant analysis (PLS-DA) were performed using the ropls package in R to visualize group separation and identify variables contributing to discrimination. Model performance was evaluated by R^2 and Q^2 values, with 200-fold permutation tests to avoid overfitting.

3 Results

3.1 Proteomic Changes in HCM Myocardium

Using a threshold of $|\log2FC| > 1$ and $p < 0.05$ (false discovery rate was not applied to the p-values, as this exploratory study prioritized sensitivity to detect potential protein changes), a total of 165 DEPs were identified between HCM and control myocardial tissue, including 100 upregulated and 65 downregulated proteins (Fig. 1A; detailed in Supplementary Table S1). Hierarchical clustering heatmaps (Fig. 1B) and OPLS-DA (Fig. 1C), together with PLS-DA (Fig. 1D), showed clear separation between groups, indicating a distinct proteomic signature in HCM.

GO enrichment analysis revealed that these proteins were predominantly localized to mitochondrial structures. The top enriched cellular component terms included "mitochondrial part", "mitochondrial membrane", and "mitochondrial inner membrane", underscoring extensive remodeling of mitochondrial compartments (Fig. 2A). Molecular function analysis highlighted NADH dehydrogenase- and oxidoreductase-related activities, further supporting disruption of electron transport and redox balance (Fig. 2B). At the biological process level, consistently, altered proteins were mainly involved in "mitochondrial ATP synthesis coupled electron transport", "oxidative phosphorylation", "respiratory electron transport chain", and "cellular respiration", indicating pervasive changes in mitochondrial energy metabolism (Fig. 3A).

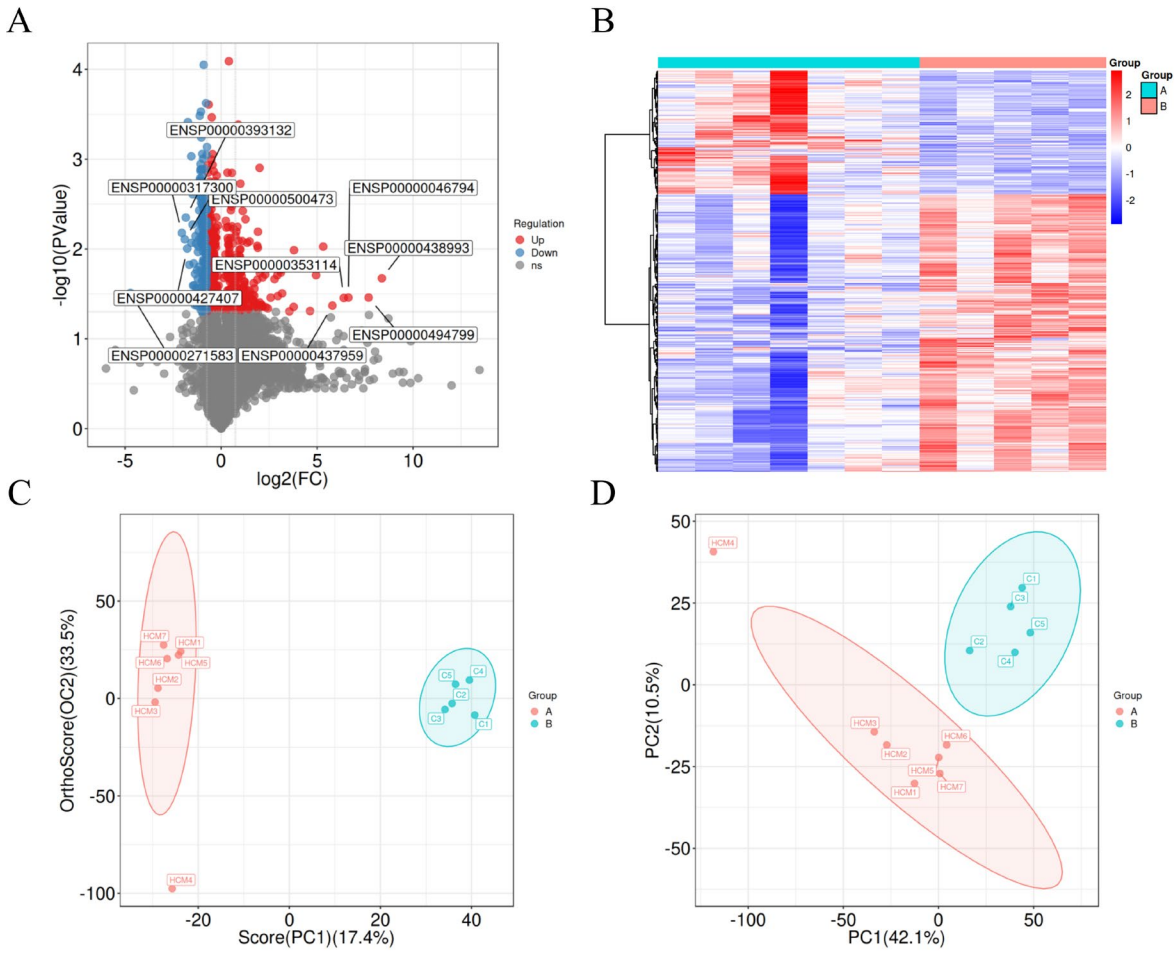

Figure 1: Differential proteomic landscape of hypertrophic cardiomyopathy versus control myocardium. (**A**) Volcano plot of differentially expressed proteins (DEPs) between hypertrophic cardiomyopathy (HCM) (n = 7) and control groups (n = 5). Red dots indicate upregulated proteins and blue dots indicate downregulated proteins (|log2FC| > 1, $p < 0.05$). (**B**) Heatmap of DEPs showing hierarchical clustering of HCM and control samples based on normalized protein expression. Each column represents a sample and each row a protein; colors reflect relative expression levels (red, higher; blue, lower). (**C**) OPLS DA score plot illustrating separation between HCM and control samples based on proteomic profiles. (**D**) PLS DA score plot showing group discrimination between HCM and control samples. In all multivariate analyses, each point represents one myocardial sample. PC, principal component; HCM, hypertrophic cardiomyopathy; DEP, differentially expressed protein; log2FC, log2 fold change; OPLS DA, orthogonal partial least squares discriminant analysis; PLS DA, partial least squares discriminant analysis.

KEGG pathway analysis was in line with these observations (Fig. 3B). Results were detailed in Supplementary Table S2. Differential proteins were significantly enriched in “Oxidative phosphorylation”, “Carbon metabolism”, “Metabolic pathways”, “Fatty acid degradation” and “Fatty acid metabolism”, pointing to coordinated remodeling of central energy and substrate utilization pathways. In addition, enrichment in “Cardiac muscle contraction” and “Hypertrophic cardiomyopathy” links these metabolic alterations to structural and functional remodeling of the myocardium.

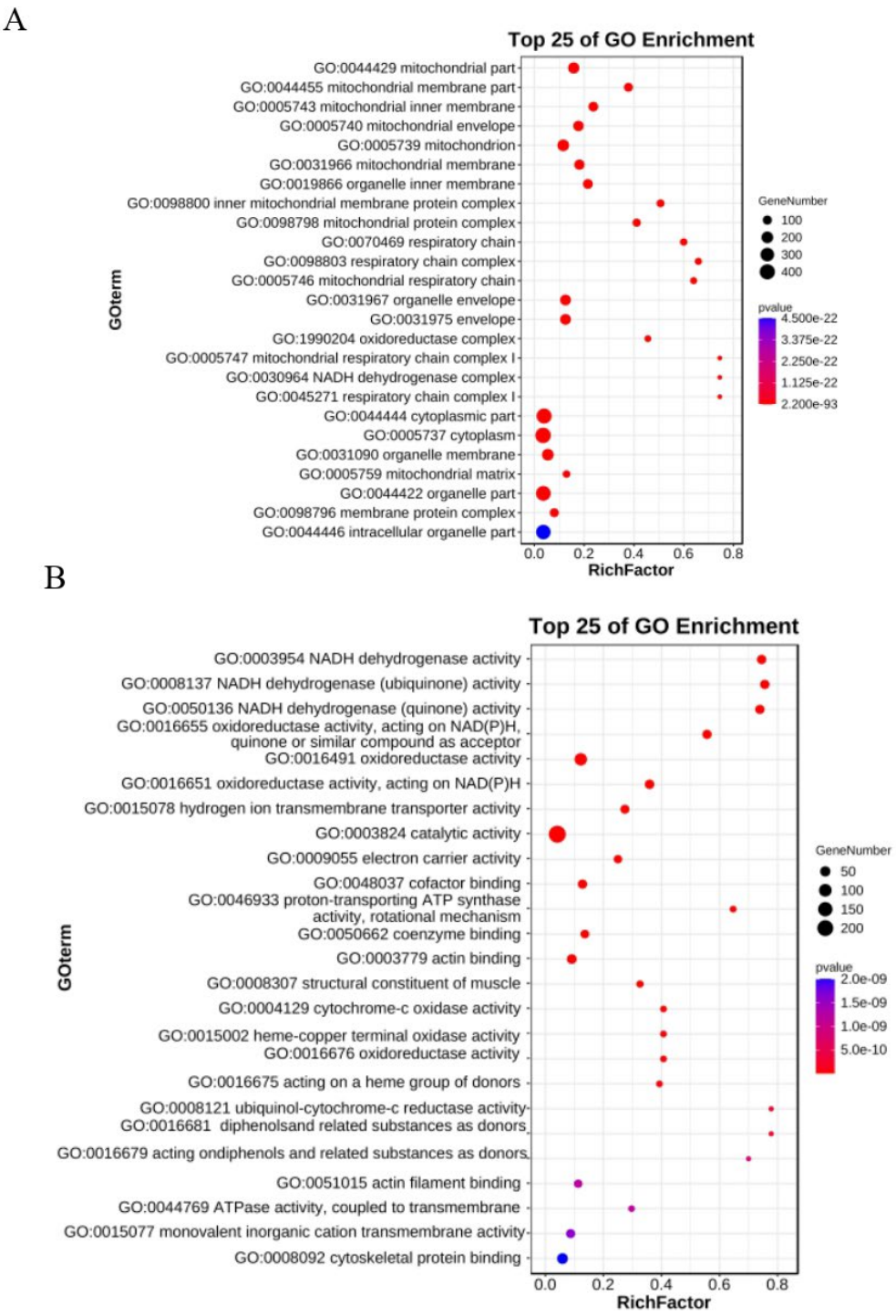

Figure 2: GO enrichment of differentially expressed proteins in HCM myocardium. (**A**) Enriched cellular component (CC) terms, highlighting mitochondrial-related structures such as mitochondrial part, mitochondrial membrane and mitochondrial inner membrane. (**B**) Enriched molecular function (MF) terms, mainly involving NADH dehydrogenase and oxidoreductase activities. Color gradients indicate the significance level of enrichment (adjusted *p*-values), and bubble size reflects the number of DEPs annotated to each term. DEP, differentially expressed protein; HCM, hypertrophic cardiomyopathy; GO, gene ontology; CC, cellular component; MF, molecular function.

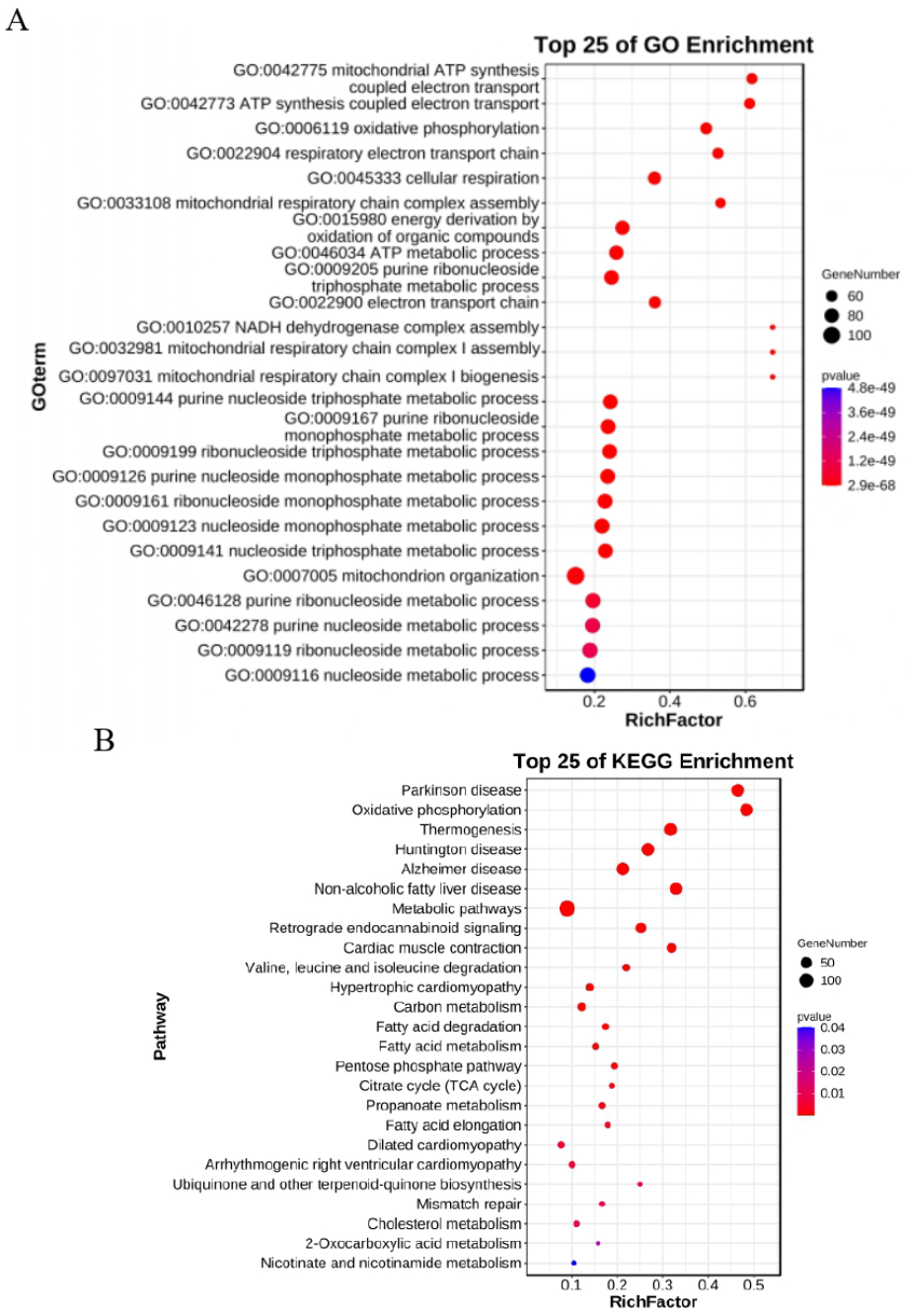

Figure 3: Biological process and KEGG pathway enrichment of differentially expressed proteins in HCM myocardium. (**A**) Gene Ontology biological process (GO-BP) enrichment, showing significant enrichment in mitochondrial and energy metabolism–related processes, including oxidative phosphorylation, respiratory electron transport chain, mitochondrial ATP synthesis coupled electron transport, and cellular respiration. (**B**) KEGG pathway enrichment analysis of DEPs, highlighting pathways associated with mitochondrial oxidative phosphorylation, carbon metabolism, fatty acid metabolism/degradation and hypertrophic cardiomyopathy. In both panels, color gradients represent the significance level of enrichment (e.g., adjusted *p*-values), and bubble size reflects the number of DEPs mapped to each term or pathway. DEP, differentially expressed protein; HCM, hypertrophic cardiomyopathy; GO-BP, gene ontology biological process; KEGG, Kyoto encyclopedia of genes and genomes.

Together, these proteomic findings suggest that HCM myocardium is characterized by pronounced mitochondrial and metabolic reprogramming, particularly affecting oxidative phosphorylation, fatty acid utilization, and contractile function, providing a mechanistic basis for subsequent metabolomic and integrative analyses.

3.2 Metabolomic Remodeling in HCM Myocardium

Untargeted metabolomic profiling identified extensive metabolic alterations in HCM myocardium compared with controls. In positive ion mode, 93 differential metabolites were detected (50 upregulated and 43 downregulated) (Fig. 4A), and in negative ion mode, 98 differential metabolites were identified (60 upregulated and 38 downregulated), based on predefined thresholds (Fig. 4B). Results were detailed in Supplementary Table S3. OPLS-DA (Fig. 4C,D), together with hierarchical clustering heatmaps (Fig. 4E), showed clear separation between HCM and control samples, indicating a distinct metabolic signature associated with HCM.

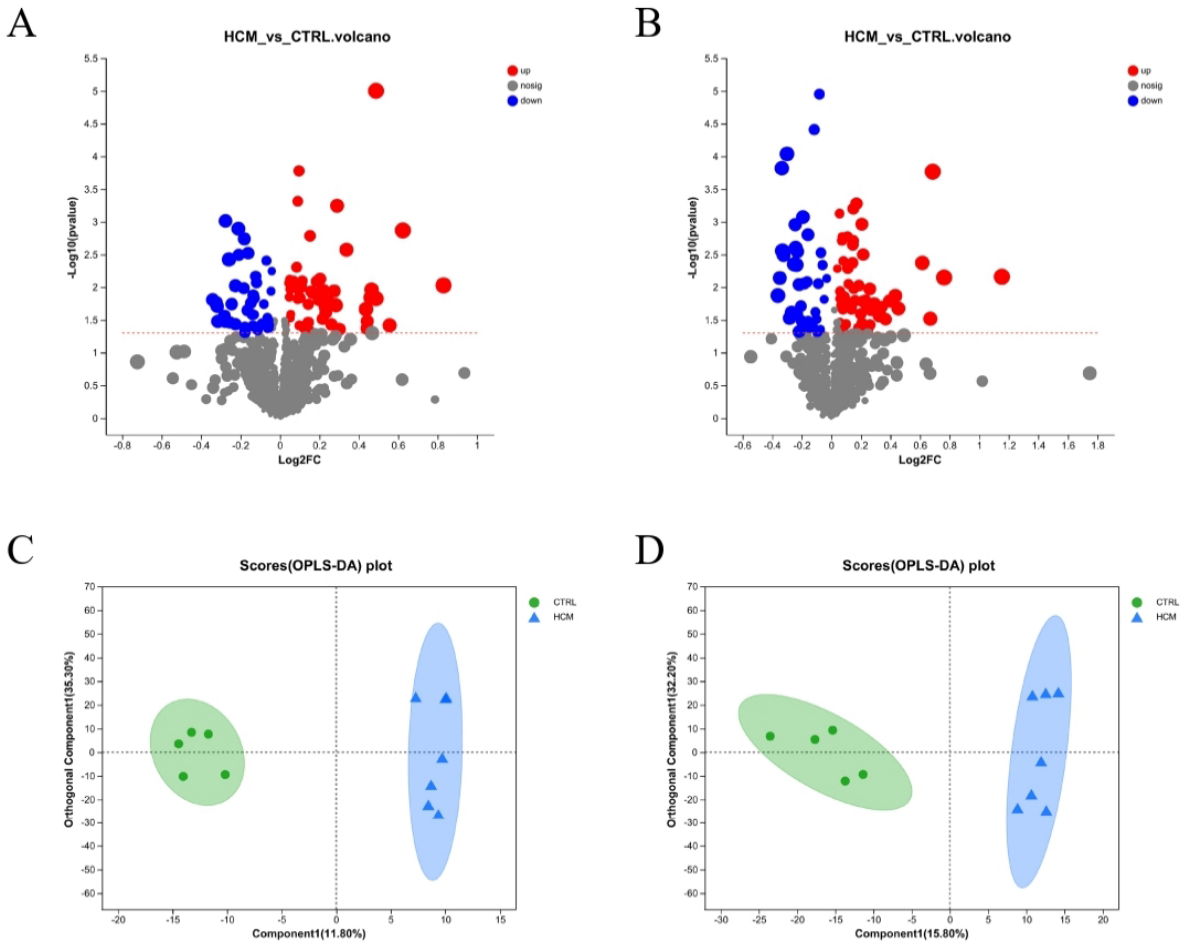

Figure 4: *Cont.*

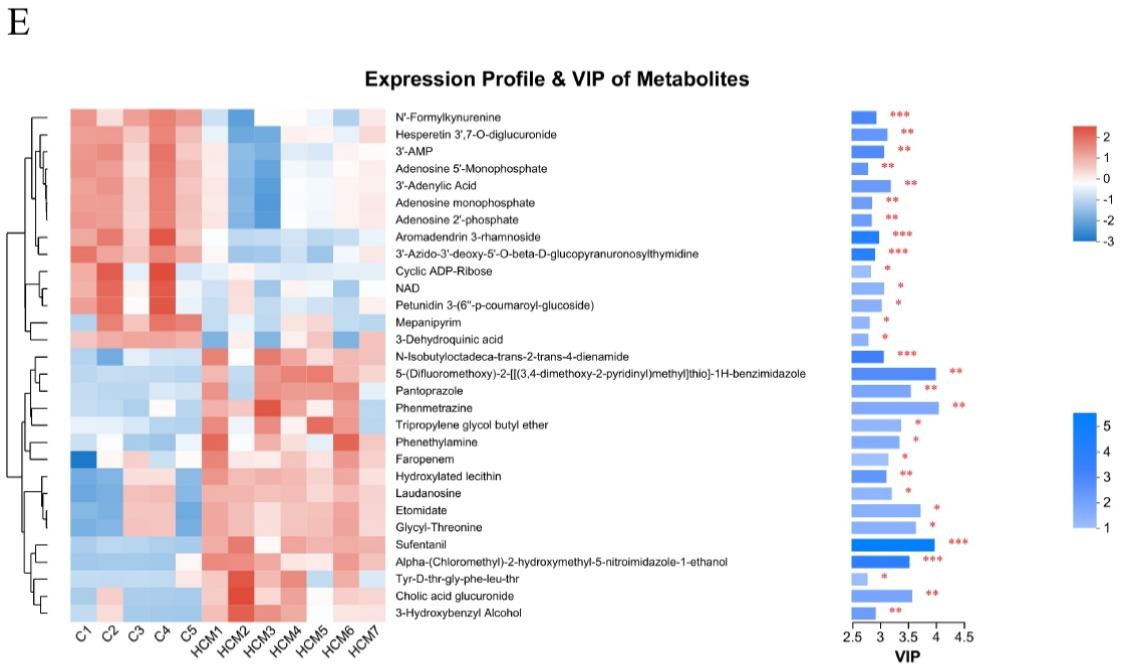

Figure 4: Overview of differential metabolomic profiles in hypertrophic cardiomyopathy (HCM) versus control myocardium. (**A**) Volcano plot of differential metabolites in positive ion mode, showing significantly upregulated (red) and downregulated (blue) metabolites. (**B**) Volcano plot of differential metabolites in negative ion mode. (**C**,**D**) OPLS-DA score plots for positive ion mode (**C**) and negative ion mode (**D**), illustrating clear separation between HCM and control samples based on metabolite profiles. (**E**) Hierarchical clustering heatmap of differential metabolites with variable importance in projection (VIP) scores, showing distinct clustering of HCM and control groups. In all multivariate analyses, each point represents one myocardial sample. Differential metabolites were defined by predefined thresholds (e.g., |log2FC| and *p*-value/VIP). HCM, hypertrophic cardiomyopathy; OPLS-DA, orthogonal partial least squares-discriminant analysis; VIP, variable importance in projection. $^{*}p < 0.05$, $^{**}p < 0.01$, $^{***}p < 0.001$.

KEGG enrichment analysis of differential metabolites ($p < 0.05$) highlighted several pathways related to energy metabolism, nucleotide turnover and signaling regulation (Fig. 5A). Results are detailed in Supplementary Table S4. Notably, “Purine metabolism” and “Pantothenate and CoA biosynthesis” were enriched, suggesting altered high-energy phosphate handling and CoA-dependent metabolic processes. Pathways such as “Glycerophospholipid metabolism” and “Choline metabolism” pointed to remodeling of membrane lipid composition. In addition, several signaling and stress-related pathways were significantly enriched, including the “AMPK signaling pathway”, “cGMP-PKG signaling pathway”, and “FoxO signaling pathway”, which are closely linked to cellular energy sensing, survival and stress adaptation (Fig. 5B). The presence of “Oxidative phosphorylation” and “Thermogenesis” among enriched pathways further supports the notion of mitochondrial functional reprogramming, consistent with our proteomic findings (Fig. 5B).

Collectively, these metabolomic changes suggest that HCM myocardium undergoes coordinated alterations in nucleotide, lipid, and amino acid metabolism, together with disruption of energy-sensing and mitochondrial pathways, providing a metabolic context for the proteomic evidence of impaired oxidative phosphorylation and mitochondrial remodeling. These metabolic changes, particularly those related to oxidative phosphorylation and energy-sensing pathways, prompted us to perform an integrated proteomic–metabolomic pathway analysis.

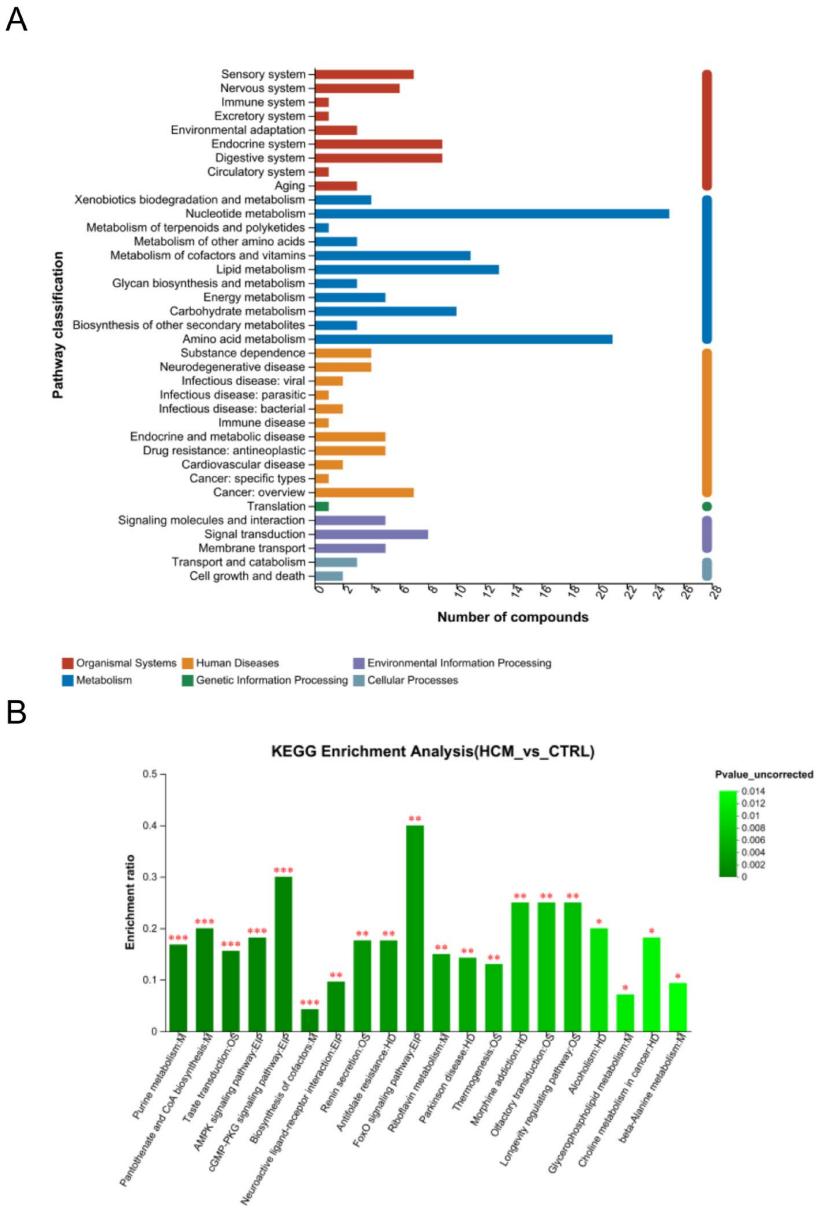

Figure 5: KEGG pathway enrichment of differential metabolites in HCM myocardium. (**A**) Bar plot of KEGG pathway classification for significantly enriched pathways, summarizing the main functional categories of differential metabolites. (**B**) KEGG pathway enrichment plot of differential metabolites, with color depth (green) indicating the significance level (darker color represents smaller p-values). HCM, hypertrophic cardiomyopathy; KEGG, Kyoto encyclopedia of genes and genomes. $^{*}p < 0.05$, $^{**}p < 0.01$, $^{***}p < 0.001$.

3.3 Integrated Proteomic–Metabolomic Pathway Analysis

To identify pathways that were consistently perturbed at both the protein and metabolite levels, we intersected the KEGG enrichment results from proteomics (77 pathways with $p < 0.05$) and metabolomics (38 pathways with $p < 0.05$). This analysis yielded seven overlapping pathways: “Purine metabolism”, “cGMP-PKG signaling pathway”, “Parkinson disease”, “Thermogenesis”, “Sulfur metabolism”, “Oxidative phosphorylation”, and “Retrograde endocannabinoid signaling”. These shared pathways highlight biological processes in which enzyme expression and metabolite abundance are simultaneously altered (Fig. 6A).

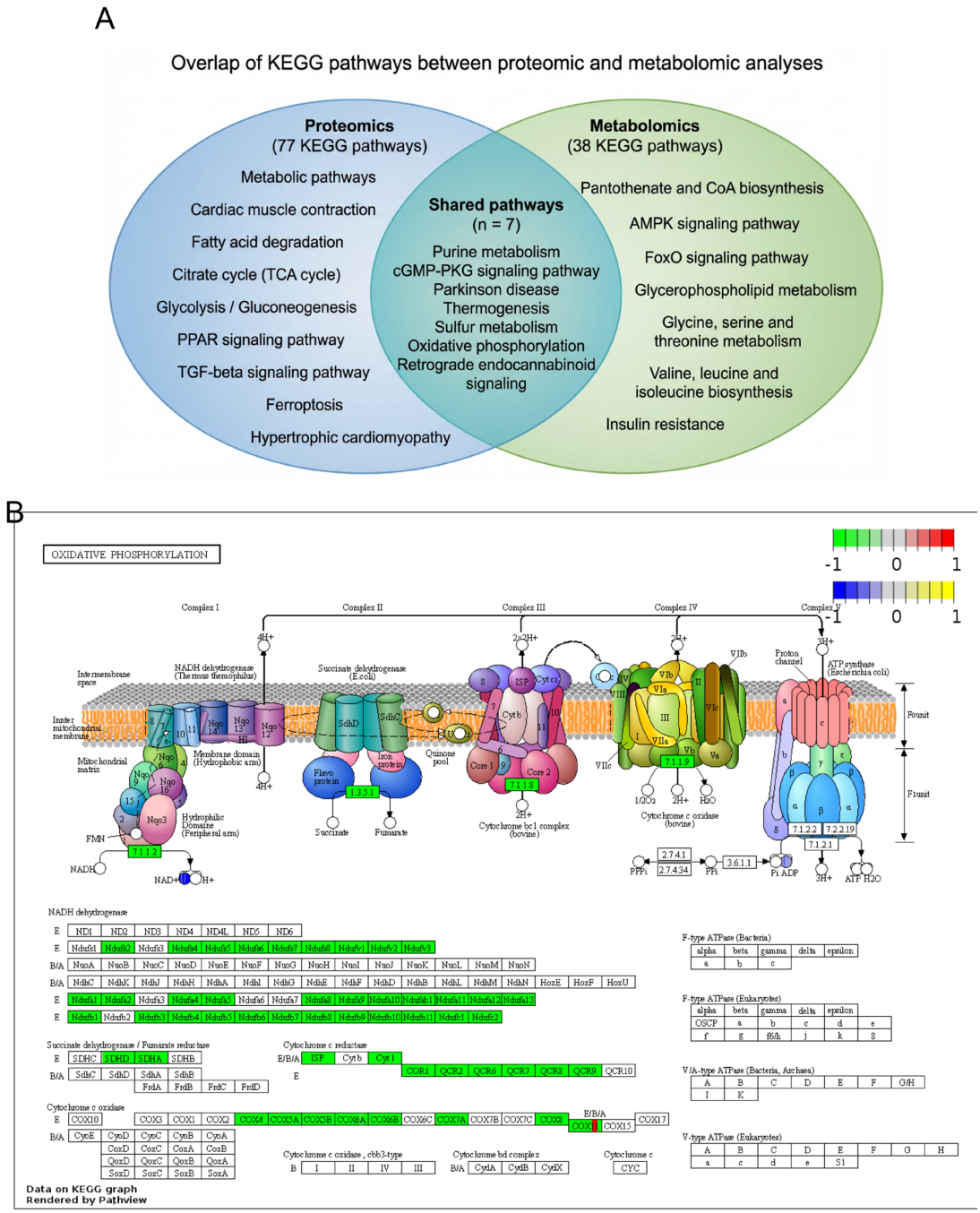

Figure 6: Integrated proteomic–metabolomic pathway analysis highlighting oxidative phosphorylation in HCM myocardium. (**A**) Venn diagram showing the overlap between significantly enriched KEGG pathways in proteomic (77 pathways) and metabolomic (38 pathways) analyses. (**B**) KEGG oxidative phosphorylation pathway map generated by Pathview, integrating differentially expressed proteins and metabolites. Downregulated proteins are indicated in green; only ATP5PO, a subunit of ATP synthase (complex V) is indicated in red, and significantly decreased metabolites (e.g., NAD and ADP) are highlighted in blue, illustrating coordinated impairment of mitochondrial electron transport and ATP production in HCM myocardium. HCM, hypertrophic cardiomyopathy; KEGG, Kyoto encyclopedia of genes and genomes.

3.4 Integrated Alterations in the Oxidative Phosphorylation Pathway

Given its multi-omics support and central relevance to myocardial energy production, we further examined the oxidative phosphorylation pathway in detail. In total, 24 DEPs mapped to this pathway. Strikingly, 23 of these proteins were downregulated in HCM myocardium compared with controls, whereas only ATP5PO, a subunit of ATP synthase (complex V), was upregulated. This pattern suggests a broad suppression of electron transport chain components accompanied by a relative increase in a single ATP synthase subunit, consistent with a globally impaired but potentially compensatory regulated oxidative phosphorylation system.

At the metabolite level, two key intermediates associated with mitochondrial energy metabolism, NAD and ADP, were both significantly decreased in HCM samples. The concomitant downregulation of multiple complex I–IV proteins together with reduced levels of NAD, a critical electron carrier, and ADP, a substrate for ATP synthase, indicates that both electron transfer capacity and ATP production potential are compromised. When DEPs and metabolites were mapped onto the oxidative phosphorylation pathway, the coordinated changes in respiratory chain subunits and energy-related metabolites outlined a consistent picture of impaired mitochondrial oxidative phosphorylation in HCM myocardium (Fig. 6B).

These integrated proteomic and metabolomic alterations in the oxidative phosphorylation pathway provide mechanistic support for mitochondrial dysfunction as a key feature of HCM, and link structural changes in respiratory complexes to functional deficits in high-energy phosphate turnover.

4 Discussion

HCM has long been regarded as a disease of impaired energetics and mitochondrial dysfunction, but most previous evidence has come from non-invasive imaging, isolated metabolic measurements, or single-omics studies [10–12]. Comprehensive proteomic–metabolomic profiling of human HCM myocardium remains scarce. In this study, by combining quantitative proteomics and untargeted metabolomics on the same myocardial samples, we provide convergent multi-layer evidence that HCM myocardium is characterized by marked mitochondrial and energetic remodeling. At the proteomic level, we observed widespread downregulation of mitochondrial and oxidative phosphorylation–related proteins, together with enrichment of pathways linked to fatty acid metabolism. At the metabolomic level, we found coordinated alterations in purine metabolism, CoA-related pathways, as well as energy-sensing pathways. Importantly, integrated analysis identified seven pathways that were simultaneously enriched in both datasets, with oxidative phosphorylation emerging as the most prominent shared node, which was consistent with impaired mitochondrial ATP production. Thus, beyond cataloguing differential proteins or metabolites, our study fills an important gap by showing that mitochondrial oxidative phosphorylation dysfunction in HCM is supported at both the enzyme and metabolite levels in human myocardium.

Focusing on the oxidative phosphorylation pathway, we found that 24 DEPs mapped to this pathway, of which 23 were downregulated in HCM myocardium, while only the ATP synthase subunit ATP5PO was upregulated. This pattern suggests a broad suppression of respiratory chain complexes with a relative increase in one component of complex V. At the metabolite level, both NAD and ADP were significantly decreased in HCM samples. NAD is a key electron carrier feeding complex I [13], whereas ADP is the substrate for ATP synthase [14]; their simultaneous reduction indicates that the electron transfer capacity and the driving force for ATP synthesis are both compromised [15]. Together, the coordinated downregulation of multiple oxidative phosphorylation proteins and depletion of NAD and ADP are consistent with impaired mitochondrial ATP production in HCM myocardium.

These findings are in line with previous reports of reduced phosphocreatine/ATP ratio, decreased energetic reserve, and structural abnormalities of mitochondria in HCM and other forms of cardiac hypertrophy [16,17]. Our multi-omics data extend these observations by showing that the energetic deficit is not only reflected at the level of high-energy phosphate metabolites but is also underpinned by widespread downregulation of electron transport chain components and disturbed cofactor availability. The upregulation of ATP5PO might represent a dysregulated or insufficient compensatory response attempt to maintain ATP synthase capacity in the face of upstream electron transport limitations, although such compensation is unlikely to fully restore ATP production when both electron donors and ADP are reduced [18].

Beyond oxidative phosphorylation, several other pathways jointly enriched in our proteomic and metabolomic analyses, such as purine metabolism, cGMP–PKG signaling and sulfur metabolism, might further modulate myocardial energetics and remodeling in HCM. Altered purine metabolism is compatible with chronic energetic stress and might reflect increased turnover of ATP and related nucleotides [19]. Enrichment of cGMP–PKG signaling components suggests potential perturbation of cyclic nucleotide–dependent pathways known to influence myocardial relaxation, hypertrophy and fibrosis [20]. Changes in sulfur metabolism might be linked to redox homeostasis and thiol-containing amino acid handling, which are increasingly recognized as modulators of mitochondrial function and cell survival [21]. Although our study was not designed to dissect each of these pathways mechanistically, the convergent enrichment pattern supports a model in which mitochondrial oxidative phosphorylation impairment is embedded in a broader network of metabolic and signaling perturbations.

Several limitations of this work should be acknowledged. First, although the sample size in this study is relatively small, it is comparable to other myocardial tissue-based multi-omics studies due to the inherent difficulty in obtaining human heart tissue. The use of high-resolution mass spectrometry and stringent statistical thresholds helped mitigate the risk of false positives. Nevertheless, we acknowledge that the limited cohort size might affect the generalizability of the findings, and future studies with larger, independent cohorts are warranted to validate these observations. Second, due to the cross-sectional nature of this study, the observed associations between protein and metabolite alterations do not imply causality. While our integrated analysis highlights oxidative phosphorylation as a centrally perturbed pathway, causal relationships between specific protein changes and metabolic consequences remain to be tested in experimental models. Third, we focused on bulk myocardial tissue, which does not distinguish between cardiomyocytes and non-myocyte cell types; cell-type–specific contributions to the observed changes remain to be clarified. Future studies in larger cohorts and experimental models of HCM are warranted to technically validate key proteins and metabolites and to functionally interrogate the role of impaired oxidative phosphorylation. Incorporating single-cell or spatial approaches might further clarify the cell-type specificity of these metabolic alterations. Fourth, the integrative analysis primarily relied on the simple intersection of significantly enriched KEGG pathways from proteomics and metabolomics. While this approach effectively highlights pathways that are perturbed at both molecular layers, it does not consider directional consistency, effect sizes, or the internal connectivity of pathway members. More sophisticated integration strategies—such as network-based correlation analysis, pathway-level activity scoring, or Bayesian multi-omics models—could provide deeper mechanistic insight. Our current approach should therefore be considered an initial, hypothesis-generating step toward a more refined systems-level understanding of HCM metabolism.

Nonetheless, by providing convergent proteomic and metabolomic evidence of oxidative phosphorylation dysfunction and associated metabolic reprogramming, our study supports the concept that

mitochondrial energetics constitute a central vulnerability in HCM and might represent a promising target for therapeutic modulation. This integrated proteomic–metabolomic perspective strengthens the concept of HCM as a disorder of myocardial energetics and provides a systems-level framework for understanding how mitochondrial and metabolic remodeling might contribute to disease progression.

5 Conclusion

In summary, integrated proteomic and metabolomic profiling of human HCM myocardium suggested consistent remodeling of mitochondrial and energy metabolism, with oxidative phosphorylation emerging as a central, multi-layerly perturbed pathway. Most oxidative phosphorylation–related proteins were downregulated, accompanied by decreased levels of NAD and ADP, suggesting compromised electron transport and ATP production capacity. These findings highlight oxidative phosphorylation–related processes as potential targets for future mechanistic and therapeutic studies.

Acknowledgement: The data were analyzed through the free online platform of the majorbio cloud platform (cloud.majorbio.com).

Funding Statement: The authors received no specific funding for this study.

Author Contributions: Meng-Zhen Zhang, Ming Li, Peng-Ju Wen, Yue-Heng Wu: conceptualization, data curation, formal analysis, investigation, methodology, resources, writing—original draft. Ling Sun: conceptualization, project administration, supervision, writing—review and editing. All authors reviewed and approved the final version of the manuscript.

Availability of Data and Materials: All datasets generated/analyzed during this study are available from the corresponding authors on reasonable request.

Ethics Approval: This study received approval from the Ethics Committee of Guangdong Provincial People's Hospital (approval registration number: GDREC2016255H). All samples were collected with written informed consent from participants or their legal guardians. The study was conducted in accordance with the Declaration of Helsinki.

Conflicts of Interest: The authors declare no conflicts of interest.

Supplementary Materials: The supplementary material is available online at https://www.techscience.com/doi/10.32604/schd.2026.077380/s1. Table S1: Differentially expressed proteins between hypertrophic cardiomyopathy (n = 7) and control groups (n = 5); Table S2: Result of KEGG enrichment analyses conducted on the differentially expressed proteins; Table S3: Differential metabolites between hypertrophic cardiomyopathy (n = 7) and control groups (n = 5); Table S4: Result of KEGG enrichment analyses conducted on the differential metabolites.

Abbreviations

HCM	hypertrophic cardiomyopathy
DEPs	differentially expressed proteins
FDR	false discovery rate
iRT	indexed retention time
QC	quality control
GO	gene ontology
KEGG	Kyoto encyclopedia of genes and genomes
FC	fold change
PCA	principal component analysis
OPLS-DA	orthogonal partial least squares discrimination analysis
CC	cellular component

MF	molecular function
BP	biological process
VIP	variable importance in projection
LC–MS/MS	liquid chromatography-tandem mass spectrometry
timsTOF	trapped ion mobility spectrometry time-of-flight

References

1. Sikand N, Stendahl J, Sen S, Lampert R, Day S. Current management of hypertrophic cardiomyopathy. BMJ. 2025;389:e077274. [CrossRef].
2. Sequeira V, Batzner A, Maack C. Targeting mitochondria in hypertrophic cardiomyopathy. Eur Heart J. 2023;44(13):1186–8. [CrossRef].
3. Gao J, Liu M, Lu M, Zheng Y, Wang Y, Yang J, et al. Integrative analysis of transcriptome, DNA methylome, and chromatin accessibility reveals candidate therapeutic targets in hypertrophic cardiomyopathy. Protein Cell. 2024;15(11):796–817. [CrossRef].
4. Lumish HS, Sherrid MV, Janssen PML, Ferrari G, Hasegawa K, Castillero E, et al. Comprehensive proteomic profiling of human myocardium reveals signaling pathways dysregulated in hypertrophic cardiomyopathy. J Am Coll Cardiol. 2024;84(20):1999–2011. [CrossRef].
5. MoTrPAC Study Group, Lead Analysts, MoTrPAC Study Group. Temporal dynamics of the multi-omic response to endurance exercise training. Nature. 2024;629(8010):174–83. [CrossRef].
6. Ren Y, Yu G, Shi C, Liu L, Guo Q, Han C, et al. Majorbio Cloud: A one-stop, comprehensive bioinformatic platform for multiomics analyses. iMeta. 2022;1(2):e12. [CrossRef].
7. Wu T, Hu E, Xu S, Chen M, Guo P, Dai Z, et al. clusterProfiler 4.0: A universal enrichment tool for interpreting omics data. Innovation. 2021;2(3):100141. [CrossRef].
8. Kanehisa M, Furumichi M, Sato Y, Kawashima M, Ishiguro-Watanabe M. KEGG for taxonomy-based analysis of pathways and genomes. Nucleic Acids Res. 2023;51(D1):D587–92. [CrossRef].
9. Luo W, Brouwer C. Pathview: An R/Bioconductor package for pathway-based data integration and visualization. Bioinformatics. 2013;29(14):1830–1. [CrossRef].
10. Ranjbarvaziri S, Kooiker KB, Ellenberger M, Fajardo G, Zhao M, Vander Roest AS, et al. Altered cardiac energetics and mitochondrial dysfunction in hypertrophic cardiomyopathy. Circulation. 2021;144(21):1714–31. [CrossRef].
11. Iwata K, Matsuda J, Imori Y, Sekine T, Takano H. Four-dimensional flow magnetic resonance imaging reveals the reduction in turbulent kinetic energy after percutaneous transluminal septal myocardial ablation in hypertrophic obstructive cardiomyopathy. Eur Heart J. 2020;41(14):1454. [CrossRef].
12. Nollet EE, Duursma I, Rozenbaum A, Eggelbusch M, Wüst RCI, Schoonvelde SAC, et al. Mitochondrial dysfunction in human hypertrophic cardiomyopathy is linked to cardiomyocyte architecture disruption and corrected by improving NADH-driven mitochondrial respiration. Eur Heart J. 2023;44(13):1170–85. [CrossRef].
13. Migaud ME, Ziegler M, Baur JA. Regulation of and challenges in targeting NAD^+ metabolism. Nat Rev Mol Cell Biol. 2024;25(10):822–40. [CrossRef].
14. Lin H, Huang J, Li T, Li W, Wu Y, Yang T, et al. Structure and mechanism of the plastid/parasite ATP/ADP translocator. Nature. 2025;641(8063):797–804. [CrossRef].
15. Trepel JB, Chuang DM, Neff NH. Transfer of ADP-ribose from NAD to choleragen: A subunit acts as catalyst and acceptor protein. Proc Natl Acad Sci U S A. 1977;74(12):5440–2. [CrossRef].
16. Li Z, Hu O, Xu S, Lin C, Yu W, Ma D, et al. The SIRT3-ATAD3A axis regulates MAM dynamics and mitochondrial calcium homeostasis in cardiac hypertrophy. Int J Biol Sci. 2024;20(3):831–47. [CrossRef].
17. Qian K, Tang J, Ling YJ, Zhou M, Yan XX, Xie Y, et al. Exogenous NADPH exerts a positive inotropic effect and enhances energy metabolism via SIRT3 in pathological cardiac hypertrophy and heart failure. EBioMedicine. 2023;98:104863. [CrossRef].
18. Zech M, Kopajtich R, Steinbrücker K, Bris C, Gueguen N, Feichtinger RG, et al. Variants in mitochondrial ATP synthase cause variable neurologic phenotypes. Ann Neurol. 2022;91(2):225–37. [CrossRef].
19. Sahu U, Villa E, Reczek CR, Zhao Z, O'Hara BP, Torno MD, et al. Pyrimidines maintain mitochondrial pyruvate oxidation to support *de novo* lipogenesis. Science. 2024;383(6690):1484–92. [CrossRef].

20. Chen JY, Xie ZX, Dai JZ, Han JY, Wang K, Lu LH, et al. Reconstruction and analysis of potential biomarkers for hypertrophic cardiomyopathy based on a competing endogenous RNA network. BMC Cardiovasc Disord. 2022;22(1):422. [CrossRef].
21. Read AD, Bentley RE, Archer SL, Dunham-Snary KJ. Mitochondrial iron–sulfur clusters: Structure, function, and an emerging role in vascular biology. Redox Biol. 2021;47:102164. [CrossRef].